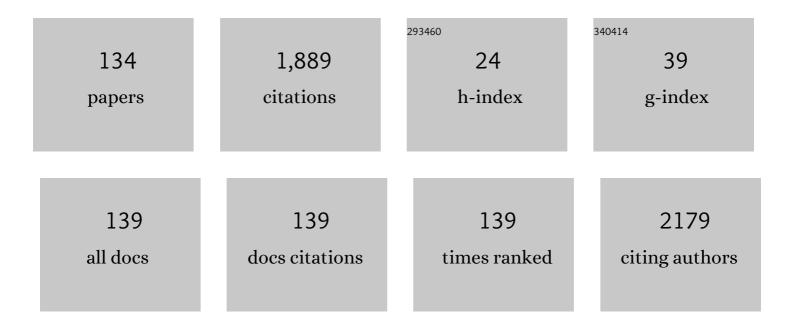
List of Publications by Year in descending order

Source: https://exaly.com/author-pdf/4888626/publications.pdf Version: 2024-02-01



#	Article	IF	CITATIONS
1	Study of Polyethylene Fibers Used in Masks Via Luminescent Aerosolized Silicon Nanoparticles. Silicon, 2022, 14, 6981-6991.	1.8	1
2	Utilizing trapped charge at bilayer 2D MoS ₂ /SiO ₂ interface for memory applications. Nanotechnology, 2022, 33, 275201.	1.3	3
3	Mechanical characterization and optical microscopy of homemade slime and the effect of some common household products. Scientific Reports, 2022, 12, 3953.	1.6	0
4	Study of Mask Fibers for Protection Against SARS-Cov-2 Via Luminescent Aerosolized Silicon Nanoparticles. ECS Transactions, 2022, 108, 3-7.	0.3	0
5	Time–thermo-dynamics of anti-Stokes and Stokes scattering and luminescence in 1-nm silicon nanoparticles: Toward an optical nanorefrigerator. AIP Advances, 2022, 12, 065219.	0.6	1
6	Evidence of Charging and Storage at the MoS ₂ /Si Interface. ECS Meeting Abstracts, 2022, MA2022-01, 881-881.	0.0	0
7	Fabrication of MoS ₂ Biosensor By Chemical Exfoliation. ECS Meeting Abstracts, 2022, MA2022-01, 2220-2220.	0.0	0
8	Study of Mask Fibers for Protection Against SARS-Cov-2 Via Luminescent Aerosolized Silicon Nanoparticles. ECS Meeting Abstracts, 2022, MA2022-01, 1099-1099.	0.0	0
9	Strong Reduction in Ge Film Reflectivity by an Overlayer of 3 nm Si Nanoparticles: Implications for Photovoltaics. ACS Applied Nano Materials, 2021, 4, 4602-4614.	2.4	10
10	Absorption in the UV-Vis Region from Chemically Exfoliated MoS2 Nanoparticles for Solar Applications. , 2021, , .		1
11	Using Conductive Atomic Force Microscopy to the Evaluate Electrical Properties of MoS2 nanoparticles for Device Applications. ECS Transactions, 2021, 104, 17-19.	0.3	0
12	Using Otsu's Method for Image Segmentation to Determine the Particle Density, Surface Coverage and Cluster Size Distribution of 3 nm Si Nanoparticles. IEEE Nanotechnology Magazine, 2021, 20, 765-774.	1.1	3
13	Polarization-based surface enhanced Raman scattering from single colloidal DNA decorated with 3Ânm silicon nanoparticles. AIP Advances, 2021, 11, .	0.6	8
14	Size dependence of charge retention in gold-nanoparticles sandwiched between thin layers of titanium oxide and silicon oxide. Applied Physics Letters, 2021, 119, .	1.5	12
15	Mechanical Characterization and Optical Microscopy of Homemade Slime and the Effect of Some Common Household Products. ECS Meeting Abstracts, 2021, MA2021-02, 1706-1706.	0.0	0
16	Using Conductive Atomic Force Microscopy to the Evaluate Electrical Properties of MoS2 nanoparticles for Device Applications. ECS Meeting Abstracts, 2021, MA2021-02, 604-604.	0.0	0
17	Tunable plasmon–polarizmon resonance and hotspots in metal–silicon core–shell nanostructures. AIP Advances, 2021, 11, .	0.6	3
18	Improved figures of merit of nano-Schottky diode by embedding and characterizing individual gold nanoparticles on n-Si substrates. Nanotechnology, 2020, 31, 125708.	1.3	18

#	Article	IF	CITATIONS
19	Modulating Surface Roughness of Low Temperature PECVD Germanium using Multilayer Drop Casting of 2.85 nm Silicon Nanoparticles. , 2020, , .		1
20	Basics of memory devices. , 2020, , 1-22.		0
21	Overview of charge trapping memory devices—Tunnel band engineering. , 2020, , 23-44.		0
22	Overview of charge trapping memory devices—charge trapping layer engineering. , 2020, , 45-66.		0
23	Atomic layer deposition based nano-island growth. , 2020, , 67-106.		0
24	Laser ablated nanoparticles synthesis. , 2020, , 107-131.		0
25	Agglomeration-based nanoparticle fabrication. , 2020, , 133-153.		1
26	Scalability of nano-island based memory devices. , 2020, , 155-174.		1
27	Time dependence of electrical characteristics during the charge decay from a single gold nanoparticle on silicon. RSC Advances, 2020, 10, 41741-41746.	1.7	3
28	Charging and discharging characteristics of a single gold nanoparticle embedded in Al2O3 thin films. Applied Physics Letters, 2020, 116, .	1.5	18
29	Photodetection Characteristics of Gold Coated AFM Tips and n-Silicon Substrate nano-Schottky Interfaces. Scientific Reports, 2019, 9, 13586.	1.6	20
30	Effect of Silver Nanoparticles on the Electrical Characteristics of Oxide/Semiconductor Heterojunctions. ECS Transactions, 2019, 89, 133-136.	0.3	2
31	Hexagonal germanium formation at room temperature using controlled penetration depth nano-indentation. Scientific Reports, 2019, 9, 1593.	1.6	24
32	Wet non-thermal integration of nano binary silicon-gold system with strong plasmonic and luminescent characteristics. AIP Advances, 2019, 9, .	0.6	7
33	Complementary metal oxide semiconductor (CMOS) compatible gallium arsenide metal-semiconductor-metal photodetectors (GaAs MSMPDs) on silicon using ultra-thin germanium buffer layer for visible photonic applications. Journal of Applied Physics, 2019, 126, .	1.1	11
34	III-V/Si dual junction solar cell at scale: Manufacturing cost estimates for step-cell based technology. Journal of Renewable and Sustainable Energy, 2018, 10, .	0.8	18
35	High performance graphene-silicon Schottky junction solar cells with HfO2 interfacial layer grown by atomic layer deposition. Solar Energy, 2018, 164, 174-179.	2.9	47
36	Interface engineering of graphene–silicon Schottky junction solar cells with an Al ₂ O ₃ interfacial layer grown by atomic layer deposition. RSC Advances, 2018, 8, 10593-10597.	1.7	27

#	Article	IF	CITATIONS
37	Passivation of Ge/high- <i>κ</i> interface using RF Plasma nitridation. Semiconductor Science and Technology, 2018, 33, 015003.	1.0	7
38	Direct growth of thin Ge-on-Si layer at low temperature as a template for lattice matched GaAs based solar cells. , 2018, , .		0
39	Tuning the optical properties of RF-PECVD grown μc-Si:H thin films using different hydrogen flow rate. Superlattices and Microstructures, 2017, 107, 172-177.	1.4	10
40	Hydrogen-Induced Crystallization of Germanium Films at Low Temperature Using an RF-PECVD Reactor. ECS Transactions, 2017, 77, 213-217.	0.3	1
41	Germanium MOS capacitors grown on Silicon using low temperature RF-PECVD. Journal Physics D: Applied Physics, 2017, 50, 405107.	1.3	8
42	Cubic-phase zirconia nano-island growth using atomic layer deposition and application in low-power charge-trapping nonvolatile-memory devices. Nanotechnology, 2017, 28, 445201.	1.3	17
43	Corrigendum to "Comparative study of thin film n-i-p a-Si:H solar cells to investigate the effect of absorber layer thickness on the plasmonic enhancement using gold nanoparticles―[Solar Energy 120 (2015) 257–262]. Solar Energy, 2017, 153, 783.	2.9	Ο
44	Corrigendum to "Enhanced performance of thin-film amorphous silicon solar cells with a top film of 2.85 nm silicon nanoparticles―[Solar Energy 125 (2016) 332–338]. Solar Energy, 2017, 153, 784.	2.9	1
45	Toward fast growth of large area high quality graphene using a cold-wall CVD reactor. RSC Advances, 2017, 7, 51951-51957.	1.7	29
46	Low temperature deposition of germanium on silicon using Radio Frequency Plasma Enhanced Chemical Vapor Deposition. Thin Solid Films, 2017, 636, 585-592.	0.8	23
47	Distribution and coverage of 40 nm gold nano-particles on aluminum and hafnium oxide using electrophoretic method and fabricated MOS structures. Materials Research Bulletin, 2017, 86, 302-307.	2.7	1
48	Effect of atomic layer deposited Al2O3:ZnO alloys on thin-film silicon photovoltaic devices. Journal of Applied Physics, 2017, 122, .	1.1	11
49	Nanoislands-Based Charge Trapping Memory: A Scalability Study. IEEE Nanotechnology Magazine, 2017, 16, 1143-1146.	1.1	10
50	Detailed Characterization for TCAD Simulations of GaAs0.76P0.24/Si1-yGey/Si Single Junction Solar Cells. , 2017, , .		0
51	Increase in Maximum Power of a-Si, c-Si and GaAs.76P.24 Solar Cells Under Low Concentration. , 2017, , .		Ο
52	Metal-germanium-metal photodetector grown on silicon using low temperature RF-PECVD. Optics Express, 2017, 25, 32110.	1.7	45
53	Effect of mobility and band structure of hole transport layer in planar heterojunction perovskite solar cells using 2D TCAD simulation. Journal of Computational Electronics, 2016, 15, 1110-1118.	1.3	33
54	Enhancement in c-Si solar cells using 16 nm InN nanoparticles. Materials Research Express, 2016, 3, 056202.	0.8	6

4

#	Article	IF	CITATIONS
55	Theoretical efficiency limit for a two-terminal multi-junction "step-cell―using detailed balance method. Journal of Applied Physics, 2016, 119, .	1.1	19
56	~3-nm ZnO Nanoislands Deposition and Application in Charge Trapping Memory Grown by Single ALD Step. Scientific Reports, 2016, 6, 38712.	1.6	27
57	Demonstration of aluminum doped ZnO as anti-reflection coating. , 2016, , .		3
58	Growth of â ⁻¹ ⁄43-nm ZnO nano-islands using Atomic Layer Deposition. , 2016, , .		1
59	Performance of planar heterojunction perovskite solar cells under light concentration. AIP Advances, 2016, 6, .	0.6	20
60	Towards demonstration of GaAs <inf>0.76</inf> P <inf>0.24</inf> /Si dual junction step-cell. , 2016, , .		0
61	â^1⁄412% Efficiency improvement in a-Si thin-film solar cells using ALD grown 2-nm-thick ZnO nanoislands. , 2016, , .		Ο
62	Aluminum doped zinc oxide-silicon heterojunction solar cell by low temperature atomic layer deposition. , 2016, , .		8
63	Optimal finger design for low concentration thin-film c-Si solar cells. , 2016, , .		Ο
64	Impact of N2O/NH3/N2 Gas Mixture on the Interface Quality of Germanium MOS Capacitors. ECS Transactions, 2016, 75, 661-666.	0.3	1
65	1D versus 3D quantum confinement in 1–5 nm ZnO nanoparticle agglomerations for application in charge-trapping memory devices. Nanotechnology, 2016, 27, 275205.	1.3	21
66	A Study of Electrical and Optical Properties of Boron-Doped Amorphous Silicon Deposited by RF-PECVD with Different B2H6/H2 Flow Rates. ECS Transactions, 2016, 72, 301-304.	0.3	3
67	Enhanced performance of thin-film amorphous silicon solar cells with a top film of 2.85 nm silicon nanoparticles. Solar Energy, 2016, 125, 332-338.	2.9	25
68	TCAD simulation and modeling of impact ionization (II) enhanced thin film c-Si solar cells. Journal of Computational Electronics, 2016, 15, 248-259.	1.3	4
69	Tailoring the Optical Properties of Boron Doped μc-Si:H Thin Films by Changing the SiH4/H2 Ratio Using RF-PECVD Process. , 2016, , .		1
70	Two-nanometer Laser Synthesized Si-Nanoparticles for Low Power Memory Applications. , 2016, , 129-156.		0
71	Growth and characterization of GaAsP top cells for high efficiency Ill–V/Si tandem PV. , 2015, , .		7
72	Structural characterization of electric-field assisted dip-coating of gold nanoparticles on silicon. AIP Advances, 2015, 5, 097181.	0.6	4

#	Article	IF	CITATIONS
73	Reducing optical and resistive losses in graded silicon-germanium buffer layers for silicon based tandem cells using step-cell design. AIP Advances, 2015, 5, 057161.	0.6	9
74	â^¼23% increase in efficiency of 100 nm thin film a-si solar cells using combination of Si/InN and Au nanoparticles. , 2015, , .		3
75	Memory effect by charging of ultra-small 2-nm laser-synthesized solution processable Si-nanoparticles embedded in Si-Al2 O3 -SiO2 structure. Physica Status Solidi (A) Applications and Materials Science, 2015, 212, 1751-1755.	0.8	13
76	Low temperature ALD grown ZnO as emitter and TCO for a thin-film a-Si PIN solar cells. , 2015, , .		0
77	Theoretical efficiency limits of a 2 terminal dual junction step cell. , 2015, , .		4
78	MOS memory with ultrathin Al2O3-TiO2 nanolaminates tunnel oxide and 2.85-nm Si-nanoparticles charge trapping layer. , 2015, , .		2
79	MOS memory with double-layer high-Î $^{ m e}$ tunnel oxide Al2O3/HfO2 and ZnO charge trapping layer. , 2015, , .		3
80	Improved efficiency of thin film a-Si:H solar cells using combination of silver and gold plasmonic nanoparticles. , 2015, , .		2
81	Design Optimization of Single-Layer Antireflective Coating for GaAs\$_{{f 1-}{m x}}\$P\$_{m x}\$/Si Tandem Cells With \$hbox{x} = hbox{0}\$, 0.17, 0.29, and 0.37. IEEE Journal of Photovoltaics, 2015, 5, 425-431.	1.5	8
82	Enhanced non-volatile memory characteristics with quattro-layer graphene nanoplatelets vs. 2.85-nm Si nanoparticles with asymmetric Al2O3/HfO2 tunnel oxide. Nanoscale Research Letters, 2015, 10, 957.	3.1	22
83	Enhancement of polycrystalline silicon solar cells efficiency using indium nitride particles. Journal of Optics (United Kingdom), 2015, 17, 105903.	1.0	7
84	Comparative study of thin film n-i-p a-Si:H solar cells to investigate the effect of absorber layer thickness on the plasmonic enhancement using gold nanoparticles. Solar Energy, 2015, 120, 257-262.	2.9	13
85	Multilayer antireflection coating design for GaAs0.69P0.31/Si dual-junction solar cells. Solar Energy, 2015, 122, 76-86.	2.9	42
86	Enhanced Light Scattering with Energy Downshifting Using 16 Nm Indium Nitride Nanoparticles for Improved Thin-Film a-Si N-I-P Solar Cells. ECS Transactions, 2015, 66, 9-16.	0.3	9
87	Efficiency enhancement in thin-film c-Si HIT solar cells using luminescent 2.85 nm silicon nanoparticles. , 2014, , .		7
88	Low power zinc-oxide based charge trapping memory with embedded silicon nanoparticles via poole-frenkel hole emission. Applied Physics Letters, 2014, 104, 013112.	1.5	34
89	Effect of carbon diffusion on performance of thin film c-Si HIT solar cells with a-SiC passivation layer. , 2014, , .		3
90	Enhanced memory effect with embedded graphene nanoplatelets in ZnO charge trapping layer. Applied Physics Letters, 2014, 105, 033102.	1.5	32

#	Article	IF	CITATIONS
91	Design of Impact Ionization enhanced thin film c-Si HIT solar cells. , 2014, , .		1
92	Enhanced memory effect via quantum confinement in 16 nm InN nanoparticles embedded in ZnO charge trapping layer. Applied Physics Letters, 2014, 104, 253106.	1.5	27
93	2-nm laser-synthesized Si nanoparticles for low-power charge trapping memory devices. , 2014, , .		11
94	Silicon nanoparticle charge trapping memory cell. Physica Status Solidi - Rapid Research Letters, 2014, 8, 629-633.	1.2	18
95	∼10% increase in short-circuit current density using 100nm plasmonic Au nanoparticles on thin film n-i-p a-Si:H solar cells. , 2014, , .		4
96	Single junction GaAs - Ge stacked tandem cell. , 2014, , .		0
97	Novel GaAs _{0.71} P _{0.29} /Si tandem step-cell design. , 2014, , .		2
98	Effect of gold nanoparticles size on light scattering for thin film amorphous-silicon solar cells. Solar Energy, 2014, 103, 263-268.	2.9	58
99	Thin-film Si1â^'xGex HIT solar cells. Solar Energy, 2014, 103, 154-159.	2.9	43
100	UV/vis range photodetectors based on thin film ALD grown ZnO/Si heterojunction diodes. Journal of Optics (United Kingdom), 2013, 15, 105002.	1.0	22
101	A Complete Physical Germanium-on-Silicon Quantum Dot Self-Assembly Process. Scientific Reports, 2013, 3, 2099.	1.6	15
102	ITO, Si3N4 and ZnO:Al Simulation of Different Anti-reflection Coatings (ARC) for Thin Film a-Si:H Solar Cells. , 2013, , .		4
103	Thin Film c-Si Solar Cell Enhanced with Impact Ionization. , 2013, , .		1
104	Effect of the Interface States on the Key Design Parameters in c-Si HIT Solar Cells. , 2013, , .		0
105	Modeling of InAs/GaAs Quantum Dot Solar Cells. , 2013, , .		1
106	Reduction of interface traps at the amorphous-silicon/crystalline-silicon interface by hydrogen and nitrogen annealing. Solar Energy, 2013, 98, 236-240.	2.9	29
107	Effect of germanium fraction on the effective minority carrier lifetime in thin film amorphous-Si/crystalline-Si1xGex/crystalline-Si heterojunction solar cells. AIP Advances, 2013, 3, 052119.	0.6	18
108	Zinc-oxide charge trapping memory cell with ultra-thin chromium-oxide trapping layer. AIP Advances, 2013, 3, .	0.6	20

#	Article	IF	CITATIONS
109	Improved efficiency of thin film a-Si:H solar cells with Au nanoparticles. , 2013, , .		6
110	Electric-field and temperature dependence of the activation energy associated with gate induced drain leakage. Journal of Applied Physics, 2013, 113, .	1.1	26
111	Diode behavior in ultra-thin low temperature ALD grown zinc-oxide on silicon. AIP Advances, 2013, 3, .	0.6	38
112	Effect of c-Si1-xGex Thickness Grown by LPCVD on the Performance of Thin-Film a-Si/c-Si1-xGex/c-Si Heterojunction Solar Cells. Materials Research Society Symposia Proceedings, 2012, 1447, 39.	0.1	4
113	Silicon-Germanium multi-quantum well photodetectors in the near infrared. Optics Express, 2012, 20, 7608.	1.7	32
114	Si nanowire memory. , 2012, , .		0
115	Thin-Film ZnO Charge-Trapping Memory Cell Grown in a Single ALD Step. IEEE Electron Device Letters, 2012, 33, 1714-1716.	2.2	44
116	Effect of interface states (D <inf>it</inf>) at the a-Si/c-Si interface on the performance of thin film a-Si/c-Si/c-Si heterojunction solar cells. , 2012, , .		1
117	ZnO based charge trapping memory with embedded nanoparticles. , 2012, , .		0
118	Simulation of a-Si/c-GaAs/c-Si Heterojunction Solar Cells. , 2012, , .		4
119	Thin film a-Si/c-Si1â^'xGex/c-Si heterojunction solar cells with Ge content up to 56%. , 2012, , .		13
120	a-Si/c-Si1â^'xGex/c-Si heterojunction solar cells. , 2011, , .		7
121	Thin Film a-Si/c-Si _{1-x} Ge _x /c-Si Heterojunction Solar Cells: Design and Material Quality Requirements. ECS Transactions, 2011, 41, 3-14.	0.3	31
122	Silicon-Germanium multi-quantum wells for extended functionality and lower cost integration. , 2010, , .		1
123	High efficiency monolithic photodetectors for integrated optoelectronics in the near infrared. , 2009, , .		2
124	A leakage current model for SOI based floating body memory that includes the Poole-Frenkel effect. , 2008, , .		6
125	High-efficiency metal-semiconductor-metal photodetectors on heteroepitaxially grown Ge on Si. Optics Letters, 2006, 31, 2565.	1.7	64
126	High performance germanium MOSFETs. Materials Science and Engineering B: Solid-State Materials for Advanced Technology, 2006, 135, 242-249.	1.7	126

#	Article	IF	CITATIONS
127	Strain Enhanced High Efficiency Germanium Photodetectors in the Near Infrared for Integration with Si. , 2006, , .		2
128	Ge on Si by novel heteroepitaxy for high efficiency near infrared photodetection. , 2006, , .		6
129	PERFORMANCE LIMITATIONS OF Si CMOS AND ALTERNATIVES FOR NANOELECTRONICS. International Journal of High Speed Electronics and Systems, 2006, 16, 175-192.	0.3	2
130	PERFORMANCE LIMITATIONS OF SI CMOS AND ALTERNATIVES FOR NANOELECTRONICS. , 2006, , .		0
131	Ge based high performance nanoscale MOSFETs. Microelectronic Engineering, 2005, 80, 15-21.	1.1	118
132	Fabrication of high-quality p-MOSFET in Ge grown heteroepitaxially on Si. IEEE Electron Device Letters, 2005, 26, 311-313.	2.2	83
133	Effects of hydrogen annealing on heteroepitaxial-Ge layers on Si: Surface roughness and electrical quality. Applied Physics Letters, 2004, 85, 2815-2817.	1.5	146
134	Red to green rainbow photoluminescence from unoxidized silicon nanocrystallites. Journal of Applied Physics, 1998, 83, 3929-3931.	1.1	52